Vol. 191, No. 14

Survival of Pathogenic Mycobacteria in Macrophages Is Mediated through Autophosphorylation of Protein Kinase G[▽][†]

Nicole Scherr,‡ Philipp Müller,‡ Damir Perisa, Benoît Combaluzier, Paul Jenö, and Jean Pieters*

Biozentrum, University of Basel, Basel, Switzerland

Pathogenic mycobacteria survive within macrophages through the inhibition of phagosome-lysosome fusion. A crucial factor for avoiding lysosomal degradation is the mycobacterial serine/threonine protein kinase G (PknG). PknG is released into the macrophage cytosol upon mycobacterial infection, suggesting that PknG might exert its activity by interfering with host signaling cascades, but the mode of action of PknG remains unknown. Here, we show that PknG undergoes autophosphorylation on threonine residues located at the N terminus. In contrast to all other mycobacterial kinases investigated thus far, autophosphorylation of PknG was not involved in the regulation of its kinase activity. However, autophosphorylation was crucial for the capacity of PknG to promote mycobacterial survival within macrophages. These results will contribute to a better understanding of the virulence mechanisms of pathogenic mycobacteria and may help to design improved inhibitors of PknG to be developed as antimycobacterial compounds.

The genome of *Mycobacterium tuberculosis* comprises 11 serine/threonine protein kinases which are considered key players in signaling cascades by transferring phosphate groups from γ-ATP to the side chain hydroxyl group of serine and threonine residues in their substrates (1, 25). One of these kinases, protein kinase G (PknG), is secreted into the cytosol of infected macrophages and prevents the intracellular destruction of mycobacteria by blocking phagosome-lysosome fusion (30). Its essential role in mycobacterial virulence makes PknG an attractive drug target; the precise mode of action of PknG remains unclear, however (24, 30).

Kinases in general can be classified into so-called RD and non-RD kinases based on the presence of a conserved arginine (R) and aspartate (D) sequence in the catalytic loop of the kinase domain. The RD arginine interacts with the phosphorylated activation loop and controls its fold, finally resulting in the activation of kinase activity (13, 18). Interestingly, PknG is unique among mycobacterial kinases in that the critical arginine residue in the kinase domain is lacking. The fact that PknG is classified as a non-RD kinase therefore suggests the absence of autophosphorylation in the activation loop (24).

Although PknG is known to undergo autophosphorylation (14, 30), neither the localization of the autophosphorylation sites of PknG nor the importance of autophosphorylation for PknG activity is known. Here, we identify the autophosphorylation sites of PknG and provide evidence that autophosphorylation is essential for the capacity of PknG to modulate the survival of intracellularly residing mycobacteria.

MATERIALS AND METHODS

Cloning, purification, and blotting. Wild-type PknG, PknG-ΔN (residues 74 to 750) and PknG-N-term (residues 1 to 147) were amplified by PCR, whereas the PknG mutants carrying single or multiple threonine-to-alanine point mutations were obtained by site-directed mutagenesis using a QuikChange (Multi) Site-Directed Mutagenesis Kit (Stratagene). The mutations were confirmed by DNA sequence analysis.

Wild-type and PknG mutant constructs were cloned into pET15b (Novagen) using NdeI and XhoI (PknG-ΔN and PknG-N-term), NdeI and HindIII (PknG with threonine-to-alanine point mutations at T_{23}, T_{26}, T_{32}, T_{63}, T_{64}, T_{63} and T_{64} ($T_{63/64}$), $T_{23/63/64}$, $T_{26/63/64}$, $T_{32/63/64}$, $T_{23/32/63/64}$, and $T_{26/32/63/64}$), or NdeI (PknG with $T_{21/23/26/32/63/64}$) restriction sites and expressed with an N-terminal six-histidine tag from *Escherichia coli*. Purification was performed as described earlier (24). In brief, *E. coli* cultures were grown for 16 h at 22°C, harvested, and lysed using a French press. After two centrifugations and a subsequent filtration step, the protein was applied to a HisTrap Ni^{2+}-Sepharose column (GE Healthcare), followed by size exclusion chromatography. Fractions containing His-PknG were pooled and concentrated to protein concentrations of 5 to 15 µg/µl PknG.

For in vivo studies, *pknG*-ΔN and *pknG*-Pmut (in which T_{21}, T_{23}, T_{26}, T_{32}, T_{63}, and T_{64} were mutated to alanines) were inserted into the mycobacterial vector pMV361 using EcoRV and HindIII restriction sites. *Mycobacterium bovis* BCG ΔPknG (Pasteur) was transformed (electroporated) with 200 ng of plasmid DNA. Mycobacterial lysates were obtained by disrupting the cells in the presence of protease inhibitors (phenylmethylsulfonyl fluoride and complete EDTA-free protease inhibitor cocktail; Roche) using a mixer mill (type MM 300; Retsch, Germany) with 30 beads per second, in 30-s treatments for 20 min with chilling breaks. Cell debris and nonlysed cells were removed by centrifugation (10 min at $10,000 \times g$). To test expression of PknG, 5 µg of lysate was loaded on 10% sodium dodecyl sulfate-polyacrylamide gel electrophoresis (SDS-PAGE) gels.

Western blot analysis of PknG was performed according to standard protocols (3) using a rabbit polyclonal antibody against mycobacterial PknG (FB17). After the secondary antibody (goat anti-rabbit immunoglobulin G coupled to horseradish peroxidase) was applied, signals were detected using an ECL Kit (GE Healthcare).

Kinase assays. Kinase assays were performed essentially as described before (24, 30). PknG was incubated in reaction buffer containing 25 mM Tris, pH 7.5, 2 mM $MnCl_2$, and 0.5 to 1.0 µCi of [γ-^{32}P]ATP at 37°C for 30 min. If required, 2 µg of substrate was added to the reaction mixture. The reaction was stopped by addition of 5× SDS sample buffer and boiling at 95°C for 5 min. The samples were analyzed by 10% or 12.5% SDS gels, stained with Coomassie brilliant blue, dried, and analyzed by autoradiography.

Thin-layer chromatography (TLC). ^{32}P-labeled PknG was separated by SDS-PAGE and transferred to a polyvinylidene difluoride membrane. The region corresponding to ^{32}P-labeled PknG was excised and hydrolyzed in 5.7 M HCl at 110°C for 2.5 h. The hydrolyzed amino acids were dried and resuspended in 1 µl

* Corresponding author. Mailing address: Biozentrum, University of Basel, Klingelbergstrasse 70, CH 4056 Basel, Switzerland. Phone: 41 61 267 14 94. Fax: 41 61 267 21 48. E-mail: jean.pieters@unibas.ch.
‡ N.S. and P.M. contributed equally to this work.

of standard solution (0.5 mg/ml of each phosphoserine, phosphothreonine, and phosphotyrosine in buffer, pH 1.9). Samples were spotted and separated in two dimensions on cellulose TLC plates and analyzed for phospho-amino acids by ninhydrin staining for the standard and by autoradiography for hydrolyzed PknG on the same plates.

Digestion of proteins with endoproteinase Lys-C, trypsin, and endoproteinase Asp-N. Digestions of PknG were carried out in 100 mM Tris-HCl, pH 8. If required, PknG was reduced and alkylated prior to proteolysis in order to break disulfide bonds. For this, PknG was reduced in 1 mM dithiothreitol for 30 min at 50°C, followed by alkylation in 55 mM iodoacetamide for 20 min in the dark, to prevent reformation of reduced disulfide bonds. After reduction and alkylation, samples were diluted fivefold with 100 mM Tris-HCl, pH 8. Enzymes were added to a final molar ratio of 25:1 to 50:1 (trypsin), 50:1 to 100:1 (endoproteinase Lys-C), and 20:1 to 40:1 (endoproteinase Asp-N), and the reaction mixture was incubated for the indicated times at 37°C (trypsin, 2 to 12 h; endoproteinase Lys-C, 2 to 3 h; endoproteinase Asp-N, 3 to 12 h). Reactions were terminated by the addition of trifluoroacetic acid (TFA) to a 1% final concentration, and the products were centrifuged in a tabletop microcentrifuge at maximum speed for 10 min to remove insoluble material. The supernatant was transferred to a new microcentrifuge tube and either directly analyzed by mass spectrometry or frozen at $-20°C$ until further use.

Purification of peptides from proteolytic digestions by HPLC. High-performance liquid chromatography (HPLC) was used to isolate particular fragments for further analysis and subsequent proteolytic digestions. Protein digests were separated on a C_{18} solid-phase HPLC column (2.1 by 250 mm; Vydac 218TP52) in a 0.1% TFA-acetonitrile buffer system. Peptides were eluted with 60- to 75-min gradients of 0.1% TFA to 0.1% TFA–75% acetonitrile (ACN). Fractions were collected, and ACN was removed in a Speedvac prior to further analysis and subsequent proteolytic digestions.

Identification of phosphorylated peptides by MS. To identify phosphorylated peptides derived from proteolytic digest of PknG or the isolated K2 fragment (see text), the sample was loaded onto a nano-HPLC column packed with C_{18} solid-phase material that was directly coupled to an electron spray ionization mass spectrometer (ESI-MS). Peptides were eluted in a 60-min gradient from 2 to 75% buffer B (mobile phase A, 98% water, 2% ACN, and 0.1% formic acid; and mobile phase B, 20% water, 80% ACN, and 0.1% formic acid). The eluted peptides were subjected to ESI-MS, and the obtained data were manually searched for phospho-peptides.

Analysis of ^{32}P-labeled PknG. PknG was subjected to kinase assay (see "Kinase assays" above). [γ-^{32}P]ATP-labeled PknG was digested with endoproteinase Lys-C as described above, acidified by addition of TFA to a 1% final concentration, and loaded on a C_{18} solid-phase HPLC column (2.1 by 250 mm; Vydac 218TP52). Peptides were eluted using a 0.1% TFA-acetonitrile buffer system with a 75-min gradient of 0.1% TFA to 0.1% TFA and 75% acetonitrile. One-minute fractions were collected and subjected to scintillation counting to determine the relative amount of ^{32}P present in the fractions.

Confocal microscopy. Bone marrow-derived macrophages were seeded on glass slides and infected with bacteria at an optical density index of 0.05 for 1 h, followed by a 3-h chase. Cells were fixed in methanol (4 min at $-20°C$) and incubated with primary antibodies (rat anti-lysosome-associated membrane protein 1 [LAMP1] and polyclonal rabbit anti-BCG) for 40 min at room temperature, washed in phosphate-buffered saline containing 5% fetal calf serum, and then incubated with Alexa Fluor 488 or Alexa Fluor 568 (Molecular Probes) coupled to goat anti-rabbit or goat anti-mouse antibodies (Southern Biotechnology Assoc., Birmingham, AL). Coverslips were mounted in FluoroGuard antifade reagent (Bio-Rad). Slides were analyzed by using a CLSM510 META (Zeiss) connected to an Axiovert 200 microscope (Zeiss) and the software provided by the manufacturer. In three independent experiments, three sets of 100 randomized events per strain were analyzed.

Cell organelle electrophoresis. Organelle electrophoresis was essentially performed as described previously (10, 11, 28). Bone marrow-derived macrophages were infected for 3 h with mycobacteria. To remove noninternalized bacteria, cells were washed twice (centrifugation at $450 \times g$ for 7 min to collect cells), resuspended in 1 ml of buffer, and homogenized using a cell cracker. The postnuclear supernatant (from centrifugation at $240 \times g$ for 15 min) was trypsinized (25 μg/mg protein) for 5 min at 37°C, and the reaction was stopped by the addition of soybean trypsin inhibitor (625 μg per mg of protein; Calbiochem). After sedimentation of the membranes ($100,000 \times g$ for 60 min), the pellet was resuspended in 0.5 ml of homogenization buffer containing 6% Ficoll-70 (Pharmacia) and loaded in the middle of a 10 to 6% Ficoll gradient. During electrophoresis (10.4 mA for 80 min), fractions were collected to be tested for β-hexosaminidase activity and protein amount (Bradford). Cytospins were performed to analyze the presence of bacteria in the collected fractions

(12). After the fractions were pelleted on glass slides, they were fixed with paraformaldehyde and acid-fast stained (Becton Dickinson). Slides were analyzed by fluorescence microscopy in order to count the number of bacteria in the fractions.

Survival assay. Prior to infection, mycobacteria were washed twice and resuspended in bone marrow macrophage medium. Bone marrow-derived macrophages were infected with mycobacteria (optical density index of 0.05) for 1 h at 37°C. Extracellular bacteria were removed by adding amikacin (200 μg/ml), followed by a 45-min incubation at 37°C. The cells were washed and chased in bone marrow macrophage medium. After 48 h, the medium was replaced by incorporation medium containing 0.15% saponin to lyse the macrophages and [^{3}H]uracil to label mycobacterial RNA. After a 24-h incubation time at 37°C, mycobacteria were killed by NaOH-trichloroacetic acid treatment, and the RNA was harvested onto UniFilter-96 GF/C glass fiber filter plates (Packard). The recovered radioactivity was measured by liquid scintillation counting (Microplate Scintillation Counter, Packard). The experiment was performed twice with five samples per condition.

RESULTS

Autophosphorylation of PknG. Intramolecular phosphorylation of kinases is a universal mechanism for the regulation of kinase activity and the affinity toward substrates and ligands (27). To analyze PknG autophosphorylation, kinase assays using purified PknG were performed. To that end, wild-type PknG or PknG with the mutation K181M [PknG(K181M)], a kinase-dead mutant, was incubated with [γ-^{32}P]ATP for 30 min; proteins were separated by SDS-PAGE and analyzed by autoradiography. As shown in Fig. 1A, PknG readily underwent autophosphorylation while no signal was detected for PknG(K181M). To gain further insight into PknG autophosphorylation activity and to analyze the amino acids within PknG that undergo autophosphorylation, TLC was performed on radioactively labeled amino acids derived from the hydrolysis of [γ-^{32}P]ATP-labeled PknG. PknG was found to be autophosphorylated exclusively on threonine residues (Fig. 1B). To identify the precise phospho-threonine residue(s), PknG was subjected to proteolytic digestion with endoproteinase Lys-C. Endoproteinase Lys-C cleaves peptide bonds C-terminal to lysine residues, yielding relatively large peptide fragments since lysine is a low-abundance amino acid in most proteins (in PknG, 2.7%). Digested PknG was loaded onto a nano-HPLC C_{18} column directly coupled to an ESI-MS. By ESI-liquid chromatography (LC)/MS, peptides covering 97.3% of the entire PknG sequence were identified. Only one peptide of PknG, termed the K2 fragment according to the second cleaved lysine residue, was found to be phosphorylated. The ionchromatogram obtained by ESI-LC/MS showed the presence of unphosphorylated, singly, doubly, and triply phosphorylated K2 fragments, as eluted from a C_{18}-nano-HPLC column (Fig. 1C). The original MS spectrum shows the series of different m/z ratios observed for the K2 fragment and its differentially phosphorylated states (Fig. 1D). The deconvoluted spectrum results in the absolute masses and the ratio of unphosphorylated and differentially phosphorylated forms of the K2 fragment (Fig. 1E).

To independently confirm that autophosphorylation of PknG occurs exclusively on the N-terminal K2 peptide, a ^{32}P-labeled endoproteinase Lys-C digest of PknG was analyzed by separating the resulting peptides on a C_{18} solid-phase HPLC column. The collected fractions were analyzed by liquid scintillation counting to determine the relative amount of ^{32}P present in the fractions. Phosphorylated peptides were exclu-
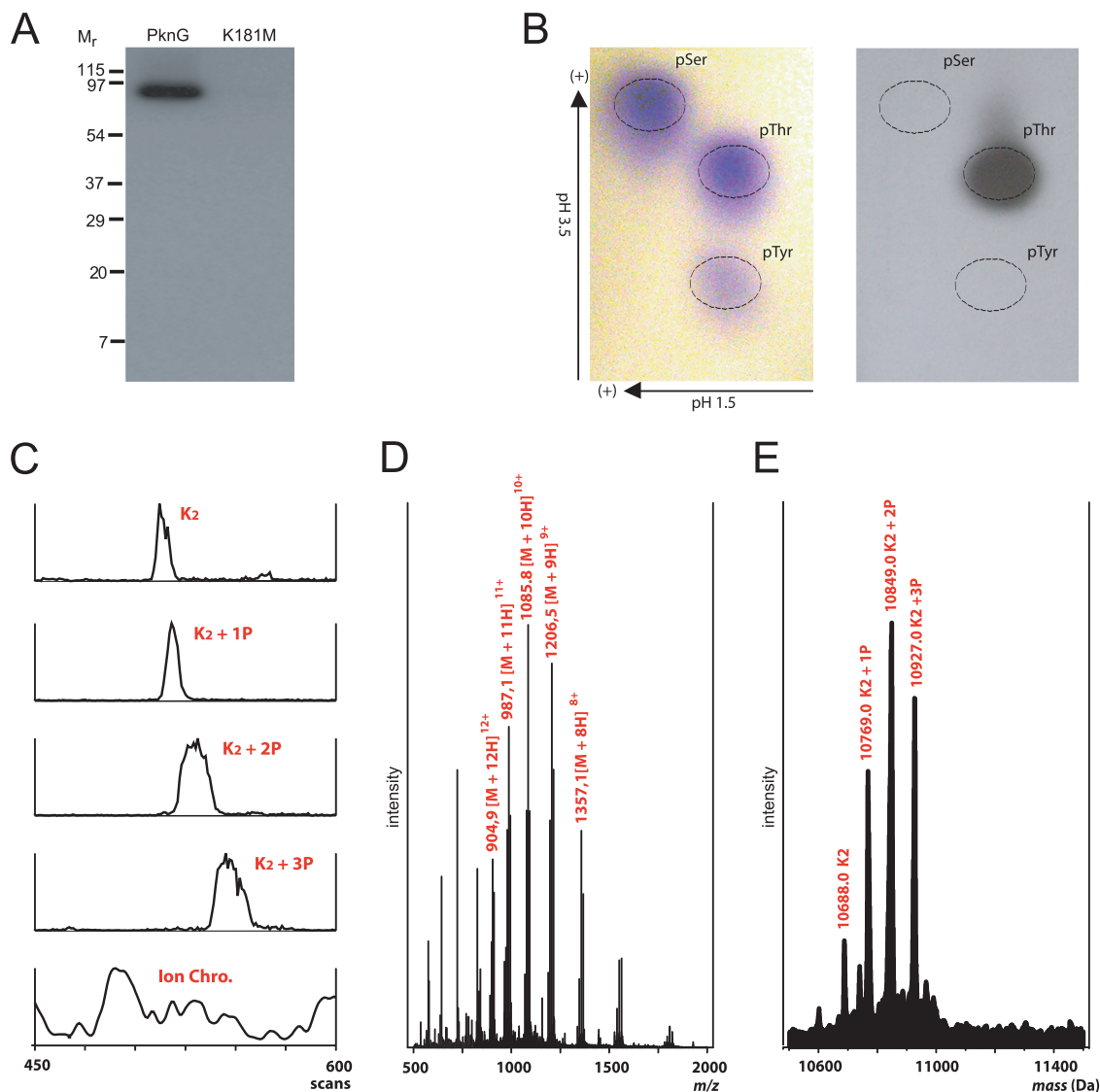
FIG. 1. Autophosphorylation of PknG. (A) Wild-type PknG or PknG(K181M) was incubated for 30 min at 37°C in kinase reaction buffer containing 1 μCi of γ-ATP. Samples were electrophoresed on a 12.5% SDS-PAGE gel and analyzed by autoradiography. M_r values are in thousands. (B) Phosphorylated PknG separated by SDS-PAGE as shown in panel A was transferred to a polyvinylidene difluoride membrane, excised, and hydrolyzed. For TLC, samples were applied to TLC cellulose plates, stained by ninhydrin, and autoradiographed. (C) Endoproteinase Lys-C-digested PknG was applied to a C_{18} nano-HPLC column coupled to the ESI-MS. The LC/MS run was further analyzed for phospho-peptides. The elution profile indicates the K2 peptide and its phosphorylated derivatives (1P to 3P) for the scan numbers between 450 to 600. (D) Original MS spectrum showing the series of different m/z ratios observed for unphosphorylated and singly, doubly, and triply phosphorylated K2 fragment. (E) Deconvoluted MS spectrum indicating the relative ratio of the unphosphorylated and the differentially phosphorylated forms of the K2 fragment. Chrom, chromatogram.

sively found in fractions 48 and 49 but not in other fractions (Fig. 2A). Analysis of fractions 48/49 by MS revealed the presence of the K2 fragment but not of other phosphorylated peptides (data not shown). Separately, peptides present in the pooled fractions 48/49 were analyzed by 16% Tricine gel electrophoresis and autoradiography, revealing the presence of a single peptide with M_r of ~11,000 (Fig. 2B) that corresponds to the size of the K2 fragment. Together, these data suggest that autophosphorylation of PknG occurs exclusively on N-terminally located threonine residues (Fig. 2C).

Identification of the autophosphorylated residues. To define the autophosphorylated amino acid residues in PknG, the K2

peptide was further fragmented by enzymatic digestion with either trypsin or endoproteinase Asp-N and analyzed by ESI-LC/MS. Tryptic digestion of the K2 fragment yielded one phospho-peptide ranging from PknG amino acid residues 10 to 60 that contained two phosphates (Fig. 3A). The endoproteinase Asp-N digestion of the K2 fragment produced two phospho-peptides, one ranging from PknG residues 18 to 38 that was doubly phosphorylated, whereas the second one ranging from PknG residues 59 to 85 was singly phosphorylated (Fig. 3A). Further fragmentation of the phospho-peptides using LC-MS/MS did not yield any further information on the localization of PknG autophosphorylation sites since the phospho-
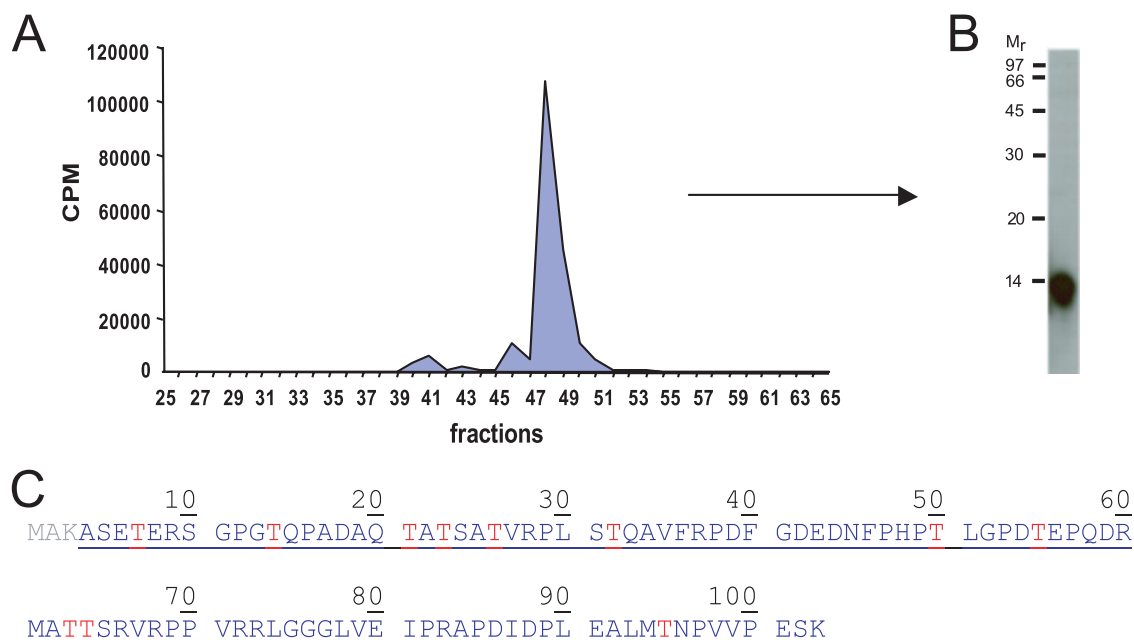
FIG. 2. Identification of the autophosphorylated PknG fragment. (A) PknG was subjected to proteolytic digestion using endoproteinase Lys-C in solution, and the digested peptides of ^{32}P-labeled PknG were separated on a C_{18} solid-phase HPLC column. Fractions were collected and analyzed by scintillation counting to determine the relative amount of ^{32}P. (B) The radioactive fractions were pooled, loaded on a 16% Tricine gel, and analyzed by autoradiography. M_r values are in thousands. (C) Sequence of the K2 ECL fragment. CPM, counts per minute.

peptides did not fragment well enough to allow for an unequivocal interpretation. Based on this analysis, six threonine residues located at the N terminus of PknG were considered as potential autophosphorylation sites (Fig. 3B).

To assign the three phosphorylation sites to the six threonine residues within the tryptic/aspartic peptides, single and multiple mutations of the corresponding threonine residues (T_{21}, T_{23}, T_{26}, T_{32}, T_{63}, and T_{64}) were introduced by site-directed mutagenesis, replacing threonine residues by alanine. The mutant proteins were expressed in *E. coli*, purified, and analyzed for phosphorylation by endoproteinase Lys-C digestion combined with ESI-LC/MS analysis and/or autoradiography.

As shown in Fig. 3C, PknG autophosphorylation was reduced when a threonine residue at either position 32 or position 63/64 is mutated into alanine. Autophosphorylation was further reduced when a second threonine residue was mutated into an alanine as demonstrated for construct $T_{32/63/64}$. Using constructs $T_{23/32/63/64}$ and $T_{26/32/63/64}$, we were able to demonstrate that autophosphorylation was completely lost for construct $T_{23/32/63/64}$, whereas the degree of autophosphorylation observed with construct $T_{26/32/63/64}$ did not change compared to construct $T_{32/63/64}$, indicating that the third phosphorylated threonine is identical with T_{23}. These results demonstrate that the major autophosphorylation sites of PknG are T_{23}, T_{32}, and $T_{63/64}$, which are located close to the N terminus (Fig. 3D). In order to minimize the risk of alternating phosphorylation of threonine residues located at a short distance from each other, a PknG mutant was constructed (termed PknG-Pmut), in which all six potential phosphorylation sites (namely, T_{21}, T_{23}, T_{26}, T_{32}, T_{63}, and T_{64}) were mutated by site-directed mutagenesis.

Analysis of PknG kinase activity in the absence of autophosphorylation. To investigate whether autophosphorylation of PknG is required for its activity, two PknG mutant proteins, PknG-Pmut and PknG-ΔN, a truncated version missing 8 kDa of the N terminus (24), were expressed and purified from *E. coli* (Fig. 4A). To analyze autophosphorylation, purified PknG wild type and PknG-ΔN as well as PknG-Pmut were subjected to a kinase reaction. As shown in Fig. 4B, no autophosphorylation signal was observed for PknG-Pmut and PknG-ΔN in contrast to PknG wild type, confirming the location of all autophosphorylation sites within the N-terminal region as specified above (Fig. 3B).

To address the question of whether autophosphorylation was involved in the regulation of kinase activity, PknG-Pmut and PknG-ΔN were incubated with an excess of PknG-N-term serving as a substrate/phospho-acceptor molecule for PknG (24). As shown in Fig. 4C, all three PknG proteins were able to phosphorylate the N-terminal fragment to a similar degree, suggesting that PknG autophosphorylation is not required for the activation of PknG kinase activity.

Role of PknG autophosphorylation on intracellular trafficking and survival of pathogenic mycobacteria. To analyze a possible role of PknG autophosphorylation in intracellular trafficking and survival of mycobacteria, *M. bovis* BCG KO-PknG (where KO is knockout) (Pasteur) strains expressing PknG-Pmut and PknG-ΔN were generated. The in vitro growth of the resulting mutant strains was similar to wild-type *M. bovis* (see Fig. S1A in the supplemental material), consistent with the earlier observed normal growth of *M. bovis* BCG lacking PknG (24, 30). In order to test expression of the mutant proteins, mycobacterial lysates were prepared and analyzed by Western blotting. Both
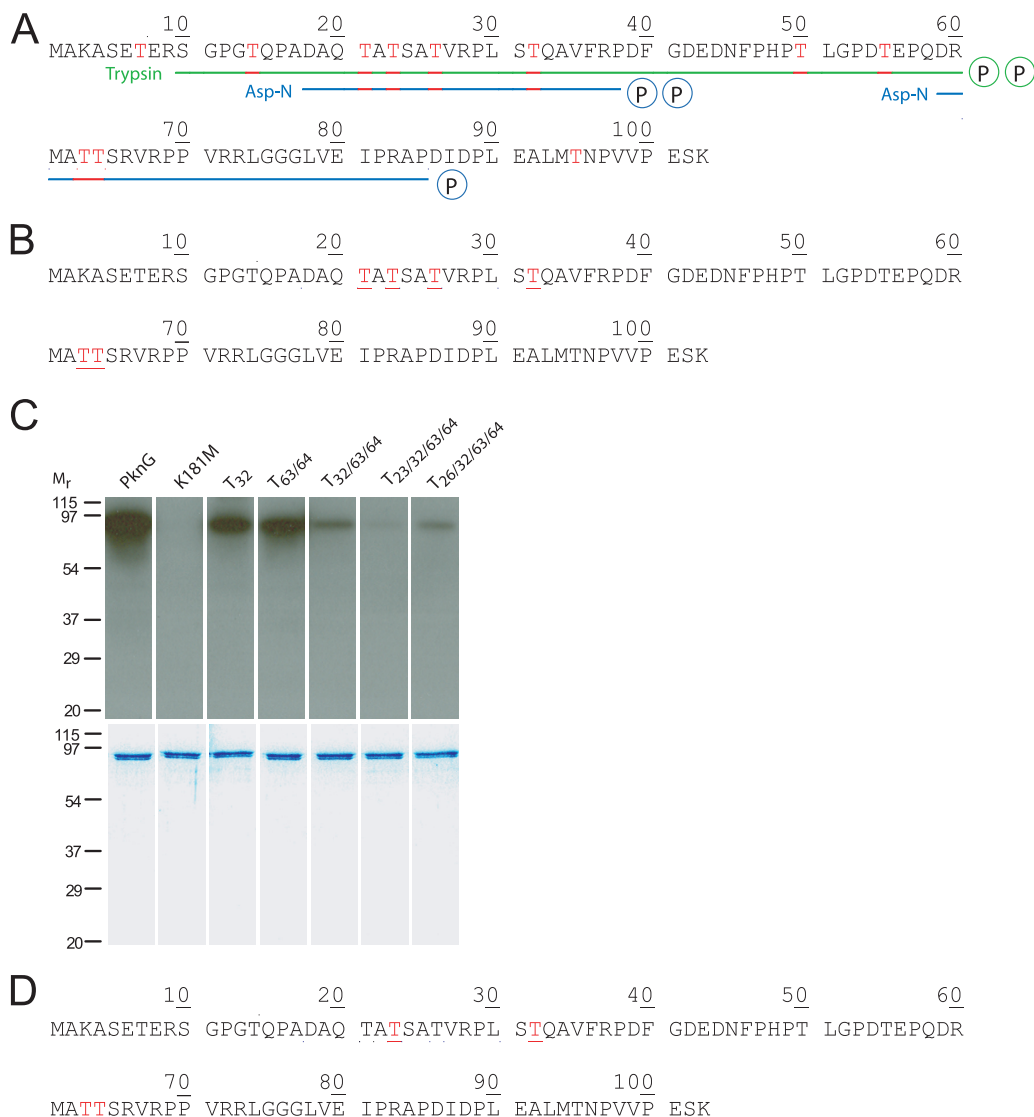
FIG. 3. Identification of the autophosphorylated residues. (A) The K2 fragment was digested with either trypsin or endoproteinase Asp-N, and the resulting peptides were identified by ESL-LC/MS. The regions covering the corresponding phospho-peptides are underlined and highlighted in green (trypsin) or blue (endoproteinase Asp-N). Threonines are highlighted in red. (B) Sequence of the K2 fragment with the potential autophosphorylation sites (T_{21}, T_{23}, T_{26}, T_{32}, T_{63}, and T_{64}) as identified in the experiments described above. Threonine residues are highlighted in red. (C) Autophosphorylation of PknG wild-type and mutant proteins containing the indicated point mutations. Kinase reaction mixtures were analyzed by 12.5% SDS-PAGE and autoradiography as well as by Coomassie staining. M_r values are in thousands. (D) Sequence of the K2 fragment with the identified autophosphorylation sites (T_{23}, T_{32}, T_{63}, and T_{64}). Threonine residues are highlighted in red.

mutant proteins, PknG-Pmut and PknG-ΔN, were expressed to the same level as wild-type PknG (see Fig. S1B in the supplemental material). Three different experimental approaches were undertaken to study the role of PknG autophosphorylation upon infection. To analyze intracellular trafficking of mycobacteria by immunofluorescence microscopy, bone marrow-derived macrophages seeded on slides were infected with the strains indicated in Fig. 5A for 1 h and chased for 3 h. The cells were fixed, washed, and stained using anti-LAMP as well as anti-*M. bovis* BCG antibodies, followed by an incubation with secondary antibodies to visualize lysosomes and mycobacterial phagosomes, respectively. The results, shown in Fig. 5B, show that for mycobacteria expressing PknG-Pmut as well as PknG-ΔN, lysosomal delivery was sig-

nificantly increased compared to wild-type mycobacteria, suggesting that autophosphorylation is essential for the prevention of mycobacterial trafficking to lysosomes.

To independently confirm the results obtained by immunofluorescence microscopy, cell organelle electrophoresis was performed. During organelle electrophoresis, lysosomes become shifted in the electric gradient, whereas mycobacterial phagosomes remain in the unshifted position (7, 12, 29), allowing the physical separation of lysosomes and phagosomes. Cells infected with the mycobacterial strains indicated were homogenized, and total organelles were subjected to electrophoresis as described in Materials and Methods. Fractions were collected and analyzed for the presence of beta-hexosaminidase (as a marker for lyso-
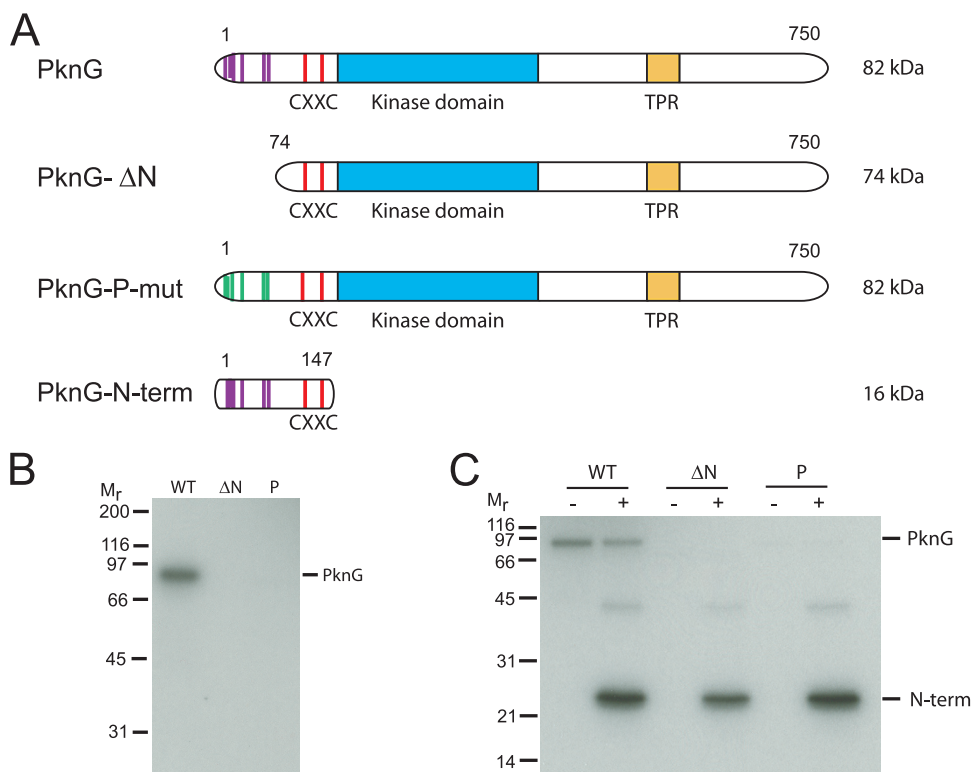
FIG. 4. Analysis of PknG autophosphorylation in vitro. (A) Domain structure of wild-type PknG, PknG-ΔN, PknG-Pmut, and PknG-N-term. PknG-ΔN lacks the first 73 amino acids at the N terminus and is devoid of all potential phosphorylation sites. For construction of the PknG-Pmut, all potential autophosphorylation sites identified were mutated to alanine residues. (B) Autophosphorylation activity of PknG wild type (WT), PknG-ΔN (ΔN), and PknG-Pmut (P). (C) Kinase activity of PknG wild type (WT), PknG-ΔN (ΔN), and PknG-Pmut (P). M_r values are in thousands. TPR, tetratricopeptide repeat.

somes), total proteins (indicating the presence of the bulk of the organelles), and acid-fast bacilli (indicating the presence of mycobacteria). While for macrophages infected with wild-type mycobacteria the bulk of the bacterial cells were found in nonshifted fractions, in macrophages infected with the PknG-Pmut and PknG-ΔN strains, a large fraction of the internalized mycobacteria were retrieved from shifted fractions, indicating their transfer to lysosomes (Fig. 5C).

The lysosomal transfer of the mycobacterial strains expressing PknG lacking the autophosphorylation sites suggests that autophosphorylation is required for intracellular survival. To directly analyze survival, macrophages were infected with *M. bovis* BCG wild type, *M. bovis* BCG-KO-PknG, *M. bovis* BCG-KO-PknG-Pmut, and *M. bovis* BCG-KO-PknG-ΔN for 1 h, after which nonphagocytosed bacteria were removed. After 48 h, the macrophages were lysed, and medium containing [³H]uracil to be incorporated into mycobacterial RNA was added to the bacteria. After 24 h of growth in labeling medium, the amount of incorporated [³H]uracil was measured by scintillation. While as expected wild-type mycobacteria were able to survive as indicated by the incorporation of [³H]uracil, none of the PknG mutant strains proliferated, as evidenced by the lack of tritium incorporation (Fig. 5D). We conclude, based upon uracil incorporation, that autophosphorylation of PknG is essential for the intracellular survival of mycobacteria within macrophages.

DISCUSSION

The virulence of pathogenic mycobacteria is dependent on their capacity to survive within macrophages by preventing phagosome-lysosome fusion (21, 22). An essential protein to block lysosomal transfer is PknG, one of the 11 eukaryotic-like serine/threonine kinases encoded in the *M. tuberculosis* genome (25, 30). The precise mechanism involved in kinase activation is important for their in vivo function. For many serine/threonine kinases, including most of the mycobacterial kinases, autophosphorylation is required for the regulation of kinase activity. We here report that for PknG kinase activity, autophosphorylation, which occurs on N-terminally located threonine residues, is fully dispensable. In contrast, autophosphorylation is essential for the capacity of PknG to block lysosomal delivery of mycobacteria. These data therefore not only separate PknG from the other serine/threonine kinases in *M. tuberculosis* but also provide important information on the mode of action of PknG in preventing mycobacterial destruction.

In other mycobacterial kinases, such as PknB, PknD, PknE, PknF, and PknH, autophosphorylation occurs on two conserved threonine residues within the activation loop (5, 23). Both the introduction of point mutations at these sites as well as treatments with mycobacterial phosphatase (PstP) resulted in inhibition of kinase activity (2), strongly suggesting auto-
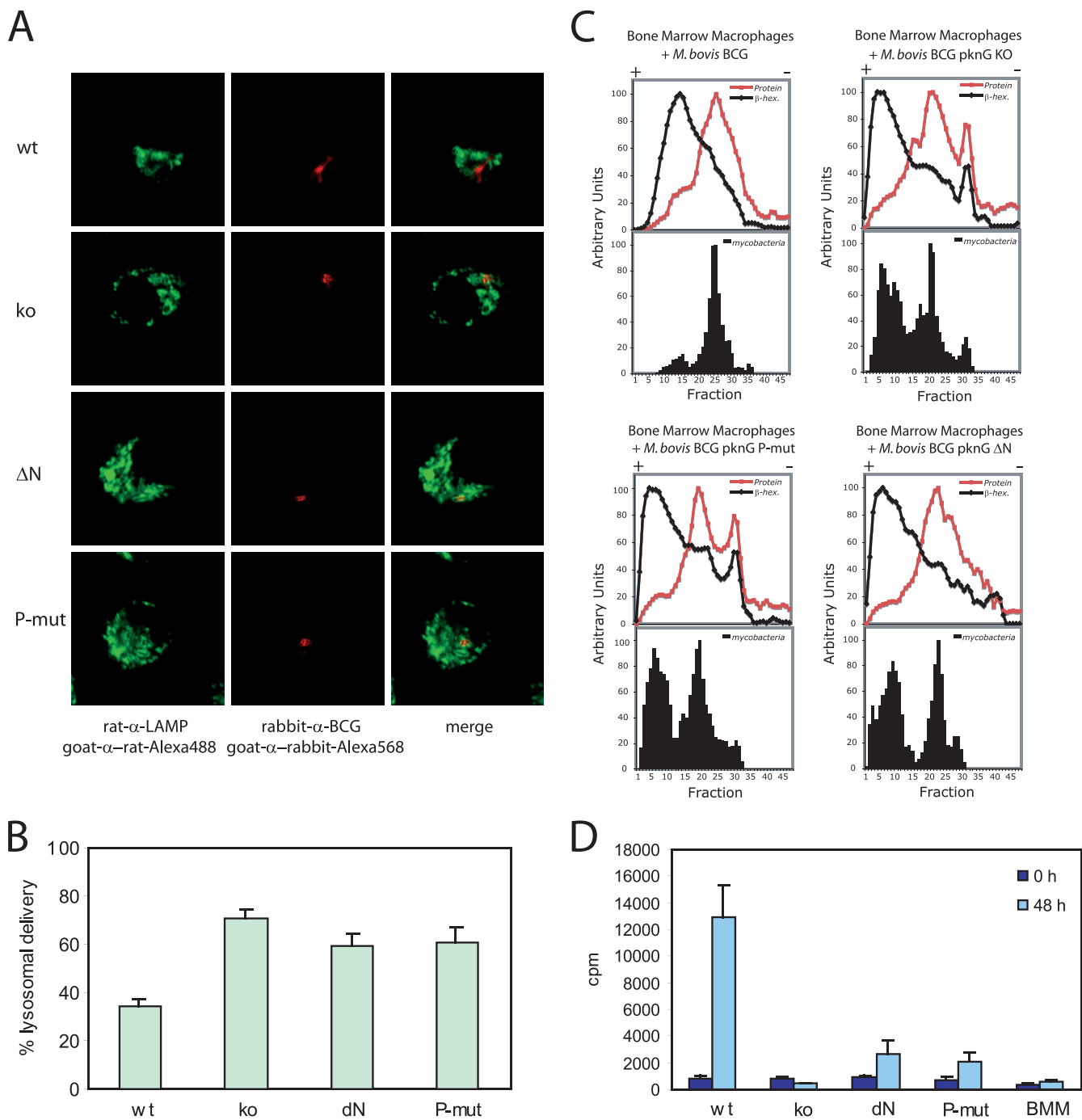
FIG. 5. Analysis of PknG autophosphorylation upon infection of macrophages. (A) Intracellular trafficking of mycobacteria analyzed by immunofluorescence microscopy. Bone marrow-derived macrophages were infected with *M. bovis* BCG wild type (wt), *M. bovis* BCG ΔPknG (ko), and *M. bovis* BCG ΔPknG overexpressing PknG-ΔN (ΔN) and PknG-Pmut (P-mut) for 1 h, followed by a 3-h chase. The infected cells were stained for lysosomes using rat anti-LAMP and for mycobacteria using polyclonal rabbit anti-BCG antibodies, visualized using Alexa Fluor 488- and Alexa Fluor 568-conjugated anti-rat and anti-rabbit antibodies, respectively, and analyzed by confocal microscopy. (B) Quantitative evaluation of the immunostaining described in panel A. *P* values of a student's *t* test (paired two sample for means) are 0.000274 for *M. bovis* BCG wild type (wt) versus *M. bovis* BCG ΔPknG (ko), 0.001595 for wild type versus *M. bovis* BCG ΔPknG overexpressing PknG-ΔN (dN), and 0.001849 for wild type versus *M. bovis* BCG ΔPknG overexpressing PknG-Pmut (P-mut). (C) Intracellular trafficking of mycobacteria analyzed by cell organelle electrophoresis. *M. bovis* BCG wild type, *M. bovis* BCG PknG knockout (ko), *M. bovis* BCG ΔPknG overexpressing PknG-Pmut, and *M. bovis* BCG ΔPknG overexpressing PknG-ΔN (ΔN) were phagocytosed for 3 h by bone marrow-derived macrophages. The cells were then washed and homogenized, and the organelles were separated by charge on a Ficoll gradient. The lysosomal fractions are represented in black, and the phagosomal fractions are shown in red. The mycobacterial repartition was determined by acid-fast staining after cytospinning of the fractions. β-hex, β-hexosaminidase. (D) Survival of internalized mycobacteria. Bone marrow-derived macrophages (BMM) were infected for 1 h with *M. bovis* BCG wild type (wt) and mutant strains (ko, dN, and P-mut as described in panel B). Extracellular bacteria were killed by amikacin treatment, and the macrophages were washed and lysed using 0.15% saponin at the indicated chase times. Mycobacterial survival was determined by bacterial incorporation of tritiated uracil for 24 h, followed by scintillation counting.

phosphorylation as the predominant activation mechanism for substrate phosphorylation. Alignment of the kinase domain demonstrated that none of these two conserved threonine residues is present in PknG (2). Furthermore, our finding that autophosphorylation is dispensable for kinase activity is consistent with PknG's being a non-RD kinase, possessing an open and extended conformation of the activation loop for which phosphorylation is not required (24).

Importantly, instead of being required for kinase activation, PknG autophosphorylation was found to be essential for its capacity to block phagosome-lysosome fusion and thereby sustain mycobacterial survival within macrophages. Since the precise signaling pathway activated by PknG within macrophages remains unknown, a role for PknG autophosphorylation remains to be established. One possibility is that PknG autophosphorylation modulates substrate binding upon PknG secretion into the macrophage cytosol (30), thereby regulating substrate phosphorylation. In particular, phosphothreonine-peptide motifs such as generated upon PknG autophosphorylation are known to be recognized by proteins containing a forkhead-associated (FHA) domain (6, 20). One FHA domain-containing protein, GarA, was recently proposed to be a substrate for mycobacterial PknG, and based on a role for GarA in glutamine metabolism, PknG was suggested to regulate glutamate metabolism (19). However, several lines of evidence argue against a role for PknG in the regulation of glutamine metabolism in vivo. First, deletion of PknG affects neither glutamine uptake nor intracellular glutamine concentrations (17). Second, growth of PknG-deficient mycobacteria is similar to the growth of wild-type bacteria under all conditions analyzed (17, 30).

Whether or not GarA phosphorylation by mycobacterial PknG occurs in vivo is unknown. Alternatively, the observed in vitro GarA phosphorylation is a result of the fact that GarA possesses an FHA domain, a well-known generic phospho-threonine-peptide recognition motif. In fact, many of the thus far identified in vivo and in vitro substrates of mycobacterial serine/threonine kinases have been shown to possess FHA domains (9, 15, 16, 25, 26). However, the genome of *M. tuberculosis* comprises only six FHA-containing proteins (4), a relatively small number in view of the whole phospho-proteome, which is supposed to encompass 500 to 1,000 phospho-Ser/phospho-Thr-containing proteins (8). Therefore, whether the substrate of PknG, which is crucial for the described function of PknG in preventing phagosome-lysosome fusion and mycobacterial survival within phagosomes, is of mycobacterial or macrophage origin remains to be determined.

The importance demonstrated here of the autophosphorylation of PknG in ensuring survival of mycobacteria within macrophages poses additional opportunities for the development of antimycobacterial drugs, for example, by targeting PknG autophosphorylation directly, thereby ensuring the effective destruction of mycobacteria within macrophage lysosomes.

ACKNOWLEDGMENTS

REFERENCES

1. **Av-Gay, Y., and M. Everett.** 2000. The eukaryotic-like Ser/Thr protein kinases of *Mycobacterium tuberculosis*. Trends Microbiol. **8:**238–244.
2. **Boitel, B., M. Ortiz-Lombardia, R. Duran, F. Pompeo, S. T. Cole, C. Cervenansky, and P. M. Alzari.** 2003. PknB kinase activity is regulated by phosphorylation in two Thr residues and dephosphorylation by PstP, the cognate phospho-Ser/Thr phosphatase, in *Mycobacterium tuberculosis*. Mol. Microbiol. **49:**1493–1508.
3. **Burnette, J.** 1981. "Western blotting": electrophoretic transfer of proteins from sodium dodecylsulfate-polyacrylamide gels to unmodified nitrocellulose and radiographic detection with antibody and radioiodinated protein A. Anal. Biochem. **112:**195–203.
4. **Cole, S. T., R. Brosch, J. Parkhill, T. Garnier, C. Churcher, D. Harris, S. V. Gordon, K. Eiglmeier, S. Gas, C. E. Barry III, F. Tekaia, K. Badcock, D. Basham, D. Brown, T. Chillingworth, R. Connor, R. Davies, K. Devlin, T. Feltwell, S. Gentles, N. Hamlin, S. Holroyd, T. Hornsby, K. Jagels, B. G. Barrell, et al.** 1998. Deciphering the biology of Mycobacterium tuberculosis from the complete genome sequence. Nature **393:**537–544.
5. **Duran, R., A. Villarino, M. Bellinzoni, A. Wehenkel, P. Fernandez, B. Boitel, S. T. Cole, P. M. Alzari, and C. Cervenansky.** 2005. Conserved autophosphorylation pattern in activation loops and juxtamembrane regions of Mycobacterium tuberculosis Ser/Thr protein kinases. Biochem. Biophys. Res. Commun. **333:**858–867.
6. **Durocher, D., and S. P. Jackson.** 2002. The FHA domain. FEBS Lett. **513:**58–66.
7. **Ferrari, G., H. Langen, M. Naito, and J. Pieters.** 1999. A coat protein on phagosomes involved in the intracellular survival of mycobacteria. Cell **97:**435–447.
8. **Greenstein, A. E., C. Grundner, N. Echols, L. M. Gay, T. N. Lombana, C. A. Miecskowski, K. E. Pullen, P. Y. Sung, and T. Alber.** 2005. Structure/function studies of Ser/Thr and Tyr protein phosphorylation in *Mycobacterium tuberculosis*. J. Mol. Microbiol. Biotechnol. **9:**167–181.
9. **Grundner, C., L. M. Gay, and T. Alber.** 2005. *Mycobacterium tuberculosis* serine/threonine kinases PknB, PknD, PknE, and PknF phosphorylate multiple FHA domains. Protein Sci. **14:**1918–1921.
10. **Hasan, Z., and J. Pieters.** 1998. Subcellular fractionation by organelle electrophoresis: separation of phagosomes containing heat-killed yeast particles. Electrophoresis **19:**1179–1184.
11. **Hasan, Z., C. Schlax, L. Kuhn, I. Lefkovits, D. Young, J. Thole, and J. Pieters.** 1997. Isolation and characterization of the mycobacterial phagosome: segregation from the endosomal/lysosomal pathway. Mol. Microbiol. **24:**545–553.
12. **Jayachandran, R., V. Sundaramurthy, B. Combaluzier, P. Mueller, H. Korf, K. Huygen, T. Miyazaki, I. Albrecht, J. Massner, and J. Pieters.** 2007. Survival of mycobacteria in macrophages is mediated by coronin 1-dependent activation of calcineurin. Cell **130:**37–50.
13. **Johnson, L. N., M. E. Noble, and D. J. Owen.** 1996. Active and inactive protein kinases: structural basis for regulation. Cell **85:**149–158.
14. **Koul, A., A. Choidas, A. K. Tyagi, K. Drlica, Y. Singh, and A. Ullrich.** 2001. Serine/threonine protein kinases PknF and PknG of *Mycobacterium tuberculosis*: characterization and localization. Microbiology **147:**2307–2314.
15. **Molle, V., L. Kremer, C. Girard-Blanc, G. S. Besra, A. J. Cozzone, and J. F. Prost.** 2003. An FHA phosphoprotein recognition domain mediates protein EmbR phosphorylation by PknH, a Ser/Thr protein kinase from *Mycobacterium tuberculosis*. Biochemistry **42:**15300–15309.
16. **Molle, V., D. Soulat, J. M. Jault, C. Grangeasse, A. J. Cozzone, and J. F. Prost.** 2004. Two FHA domains on an ABC transporter, Rv1747, mediate its phosphorylation by PknF, a Ser/Thr protein kinase from *Mycobacterium tuberculosis*. FEMS Microbiol. Lett. **234:**215–223.
17. **Nguyen, L., A. Walburger, E. Houben, A. Koul, S. Muller, M. Morbitzer, B. Klebl, G. Ferrari, and J. Pieters.** 2005. Role of protein kinase G in growth and glutamine metabolism of *Mycobacterium bovis* BCG. J. Bacteriol. **187:**5852–5856.
18. **Nolen, B., S. Taylor, and G. Ghosh.** 2004. Regulation of protein kinases; controlling activity through activation segment conformation. Mol. Cell **15:**661–675.
19. **O'Hare, H. M., R. Duran, C. Cervenansky, M. Bellinzoni, A. M. Wehenkel, O. Pritsch, G. Obal, J. Baumgartner, J. Vialaret, K. Johnsson, and P. M. Alzari.** 2008. Regulation of glutamate metabolism by protein kinases in mycobacteria. Mol. Microbiol. **70:**1408–1423.
20. **Pallen, M., R. Chaudhuri, and A. Khan.** 2002. Bacterial FHA domains: neglected players in the phospho-threonine signalling game? Trends Microbiol. **10:**556–563.
21. **Pieters, J.** 2008. Manipulation of the macrophage response by pathogenic mycobacteria. *In* S. H. E. Kaufmann and E. Rubin (ed.), Handbook of tuberculosis: molecular biology and biochemistry. Wiley-VCH, Weinheim, Germany.
22. **Russell, D. G.** 2001. *Mycobacterium tuberculosis*: here today, and here tomorrow. Nat. Rev. Mol. Cell Biol. **2:**569–577.

23. **Scheeff, E. D., and P. E. Bourne.** 2005. Structural evolution of the protein kinase-like superfamily. PloS Comput. Biol. **1:**e49.

24. **Scherr, N., S. Honnappa, G. Kunz, P. Mueller, R. Jayachandran, F. Winkler, J. Pieters, and M. O. Steinmetz.** 2007. From the cover: structural basis for the specific inhibition of protein kinase G, a virulence factor of *Mycobacterium tuberculosis*. Proc. Natl. Acad. Sci. USA **104:**12151–12156.

25. **Scherr, N., and J. Pieters.** 2009. The eukaryotic-like serine/threonine protein kinase family in mycobacteria. *In* T. Parish and A. Brown (ed.), *Mycobacterium*: genomics and molecular biology. Horizon Press, Pittsburgh, PA.

26. **Sharma, K., M. Gupta, A. Krupa, N. Srinivasan, and Y. Singh.** 2006. EmbR, a regulatory protein with ATPase activity, is a substrate of multiple serine/threonine kinases and phosphatase in *Mycobacterium tuberculosis*. FEBS J. **273:**2711–2721.

27. **Smith, J. A., S. H. Francis, and J. D. Corbin.** 1993. Autophosphorylation: a salient feature of protein kinases. Mol. Cell. Biochem. *127*-**128:**51–70.

28. **Tulp, A., D. Verwoerd, B. Dobberstein, H. L. Ploegh, and J. Pieters.** 1994. Isolation and characterization of the intracellular MHC class II compartment. Nature **369:**120–126.

29. **Tulp, A., D. Verwoerd, and J. Pieters.** 1993. Application of an improved density gradient electrophoresis apparatus to the separation of proteins, cells and subcellular organelles. Electrophoresis **14:**1295–1301.

30. **Walburger, A., A. Koul, G. Ferrari, L. Nguyen, C. Prescianotto-Baschong, K. Huygen, B. Klebl, C. Thompson, G. Bacher, and J. Pieters.** 2004. Protein kinase G from pathogenic mycobacteria promotes survival within macrophages. Science **304:**1800–1804.